Cover Page

The handle http://hdl.handle.net/1887/22644 holds various files of this Leiden University dissertation

Author: Barnier-Quer, Christophe
Title: Adjuvanted nanoparticulate seasonal influenza vaccines
Issue Date: 2013-12-04

Peptide amphiphile nanoparticles enhance the immune response against a CpG adjuvanted influenza antigen

Barnier-Quer C *, Zope H *, Bomans PHH. , Sommerdijk NAJM. , Kros A and Jiskoot W.
* Authors contributed equally

Abstract

We developed a new class of polypeptide-b-peptide amphiphiles (PbP-A), based on a hydrophilic peptide conjugated to a hydrophobic poly-γ-benzyl-L-glutamate (PBLG) block. These peptide amphiphiles are able to self-assemble into nanostructures. In this study we have shown that properties such as size, morphology and surface charge of the resulting nanoparticles can be tuned. These polypeptide nanoparticles were tested for their adjuvant capacity. Immunogenicity of the hybrid assemblies was tested in vivo and showed an improvement of the immune response for the influenza antigen co-administered with polypeptide nanoparticles or CpG containing polypeptide nanoaprticles. This advanced formulation demonstrated enhanced efficacy when compare to HA alone, or with commonly used commercial adjuvant "Alum".

Peptide and protein-derived materials have come into the spotlight for supramolecular chemists in recent years. Sequence-depending, peptides can fold into secondary structures such as β-sheets, α-helices or random coils that can further direct the hierarchical self-assembly of these macromolecules.[1] Over the last decade, self-assembly of peptide amphiphiles has been studied extensively and more recently as potential biomaterials.[2] These self-assembling peptide amphiphiles can be divided into three classes: [3] (a) amphiphilic peptides composed solely of a specific amino acid sequence [4] (b) hydrophilic peptides conjugated to a hydrophobic anchor like alkyl chains[5] and lipids,[6] and (c) hybrid peptide-polymers.[7] Conjugation of a peptide to a hydrophobic anchor strongly affects the supramolecular assembly and various morphologies have been reported, such as spherical and worm-like micelles, bicelles and vesicles.[8] These peptide amphiphile-based materials have found several potential applications in drug delivery,[9] in vivo imaging,[10] and regenerative medicine.[11] Only recently these materials have entered the field of vaccine research[12] where self-assembled peptides have been shown to enhance immune responses by acting as an adjuvant. Pioneering work by Collier and team demonstrated the capacity of self-assembling peptide motifs to provoke an immune response in mouse models against conjugated ovalbumin (OVA) peptide or protein antigens.[13] Tirrell and coworkers used peptide amphiphiles based micelles as a "self-adjuvanting" vaccine.[12] A dialkyl tail was conjugated to a peptide containing a cytotoxic T-cell epitope derived from the model tumor antigen OVA. These initial studies aimed at understanding the in vivo immune modulation using these micellar peptide-based materials. In both studies an enhanced Th2 response was observed, while the Th1 response was rather low. In our laboratory we have a long-term interest in developing effective adjuvants for influenza hemagglutinin (HA). Ideally, a viral vaccine should induce, besides antibodies, a substantial Th1 immune response, as this helps to protect against intracellular pathogens. Optimization of peptide amphiphile-based vaccines can be achieved by varying the amino acid sequence or the hydrophobic element, or by the addition of low molecular weight immune modulators.[14]

In order to improve cellular delivery, antigen-containing particles have been decorated with cell-penetrating peptides such as the TAT peptide.[15] Its arginine rich amino acid sequence results in a positive surface charge. Cationic nanoparticles (NP) generally show better efficacy for enhancing the immunogenicity of the carried antigen than neutral or negatively charged particles, presumably due to an enhanced interaction between the negatively charged cell membranes and the cationic particles.[16] [17] For example, poly(ethylene glycol)-polybutadiene polymersomes functionalized with TAT peptides successfully enhanced the cellular delivery of these NP to antigen-presenting cells (APC).[18] Furthermore, in order to enhance and modulate the immune response towards a higher Th1 response, co-delivery of an immune potentiator such as the TLR9 ligand CpG (bacterial cytosine phosphodiester guanine oligomer) is a promising approach.[19] CpG helps to

initiate a rapid innate immune response characterized by the secretion of a variety of cytokines, for example interferon-γ.[20]
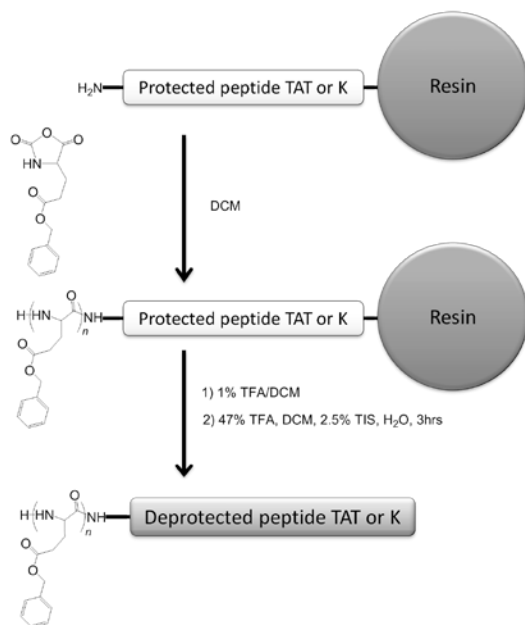

Fig. 1: Synthesis of PBLG-TAT and PBLG-K using solid phase peptide synthesis followed by N-carboxyanhydride ring-opening polymerization initiated from the N-terminal amine of the resin bound peptide.

We have previously reported a new class of polypeptide-b-peptide amphiphiles (PbP-A), based on a hydrophilic peptide block (denoted peptide "K") with a specific amino acid sequence conjugated to a hydrophobic poly-γ-benzyl-L-glutamate (PBLG) block.[14b] [21] [22] In this design peptide "K" is able to form a coiled-coil motif with the complementary peptide "E". These peptide amphiphiles self-assemble into micellar or vesicular structures depending on their composition. Control over both shape and size of the assemblies was achieved utilizing this coiled-coil motif[14b, c] The efficacy of peptide amphiphile PBLG$_{50}$-K [amino acid sequence peptide "K"; (KIAALKE)$_3$] was tested as a vaccine delivery system for an HA influenza subunit vaccine.[23] Injection of HA mixed with PBLG$_{50}$-K NP in adult mice resulted in an enhanced IgG1 antibody response against HA and an increased hemagglutination inhibition (HI) titer as compared to HA alone.[23] Unfortunately, the Th1 response remained low, as measured by the IgG2a titer. These initial results showed that the PbP-A NP might be used as an adjuvant, however a redesign is required to evoke a strong Th1 response in order to create an effective viral vaccine.

In this contribution, we aimed to design an effective vaccine containing two key features: 1) efficient delivery and uptake of the antigen (HA) by APC and 2) the incorporation of an immune potentiator that modulates the immune response towards an enhanced Th1 response. We designed PbP-A using the peptide "TAT" and peptide "K" sequence as hydrophilic head group for cellular delivery as well as to capture CpG by ionic interactions. PBLG-K was also part of this formulation enabling functionalization of the resulting NP through specific coiled coil peptide binding in future studies.[14c] PBLG-TAT and PBLG-K mixed with CpG were used to form NPs and these NPs were used to adsorb HA on the surface. This approach enables the co-delivery of the antigen together with an immune modulator aiming to induce a strong immune response.[24] The NP were examined in vitro for their capability of stimulating dendritic cells (DC) and their immunogenicity was studied in vivo by subcutaneous administration in mice and compared with that of HA formulated with aluminum salt [Al(OH)$_3$], a frequently used adjuvant in commercial vaccines.

Synthesis of the polypeptide-b-peptides was performed as shown in Fig. 1. Peptides "TAT" [Amino acid sequence: GLRKKRRQRRR] and "K" [G (KIAALKE)$_3$] were synthesized on a sieber amide resin using standard Fmoc solid phase peptide synthesis protocols. The N-terminal amine was used to initiate solid phase ring opening polymerization (ROP) of γ-benzyl-L-glutamate N-carboxyanhydride (BLG-NCA). The reaction was carried out in dichloromethane (DCM) under an inert atmosphere for two days to obtain resin-bound polypeptide-b-peptides. The resin was washed thoroughly with DCM to remove any residual homopolymers formed during the polymerization and the protected polypeptide-b-peptides were released from the solid support using 1:99 (v/v) TFA/DCM (TFA; trifluoroacetic acid) for two minutes in several fractions with subsequent precipitation in cold methanol. Polypeptide-b-peptides with high molecular weight are cleaved first and therefore macromolecules with different molecular weight can be separated. The purity of each fraction was ascertained with gel permeation chromatography (GPC) and fractions with a similar polydispersity index (PDI 1.3-1.4) and molecular weight were combined. The protecting groups were removed from the hydrophilic peptide sequence using a mixture of TFA/DCM/water/TIS (TIS; triisopropylsilane). Under the used conditions, the benzyl protecting groups of the PBLG block are unreactive. The resulting product was precipitated in cold methanol and washed several times resulting in the desired amphiphilic polypeptide-b-peptides. The removal of the protecting groups from the hydrophilic peptide and the degree of polymerization (DP) of the hydrophobic PBLG block were determined by ^{1}H-NMR analysis in DMF-d 7 at 60°C. The peak integral of the benzylic protons in the PBLG block was compared with the integral arising from the leucine and isoleucine methyl protons of the K or TAT block and revealed that the average degree of polymerization for the PBLG block was 30 for both peptide amphiphiles (PBLG$_{30}$-K and PBLG$_{30}$-TAT, Fig. S2 Supporting Information). The average molecular weights of the polymers (Table 1)

determined using ^{1}H-NMR spectroscopy are in good agreement with the data obtained by GPC.

Table 1: Molecular characteristics of the peptide compounds used in this study

Molecules	Structure[a]	M_n [g.mol^{-1}]	PDI[d]
K	G(KIAALKE)-NH$_2$	2335.8[b]	
TAT	G(LRKKRRQRRR)-NH$_2$	1508.8[b]	
PBLG$_{30}$-K	PBLG$_{30}$-G(KIAALKE)-NH$_2$	8906[c]/9912[d]	1.4
PBLG$_{30}$-TAT	PBLG$_{30}$-G(LRKKRRQRRR)-NH$_2$	8079[c]/10301[d]	1.3

[a] The sequence for the peptide "K" and "TAT" are written using the one letter amino acid code. PBLG; poly(γ-benzyl L-glutamate). [b] Determined by MALDI-TOF mass spectrometry. [c] Determined by comparing ^{1}H NMR spectroscopy. [d] Determined for protected polypeptides using GPC calibrated with polystyrene standards.

Peptide amphiphile NP were prepared by the rapid water addition-solvent evaporation (WASE) method,[22] as this procedure is fast and has been proven to be compatible with in vivo applications.[23] Four NP formulations were designed with different physicochemical properties (Table 2). Two formulations, NP1 and NP2, were composed of PBLG$_{30}$-K and PBLG$_{30}$-TAT, respectively. The third formulation, NP3, consisted of a PBLG$_{30}$-TAT:PBLG$_{30}$-K (9:1) mixture, combining peptide "TAT" to enhance cellular uptake and peptide "K". Moreover, this will enable future modification of the NP through coiled-coil formation with the complementary peptide "E", allowing further surface functionalization if desired.[7c] The 9:1 molar ratio of peptide amphiphiles PBLG$_{30}$-TAT:PBLG$_{30}$-K was selected after an initial screen by zeta potential and dynamic light scattering (DLS) measurements, which revealed that it is the most cationic mixture of all formulations that assembled into NP with reproducible size (data not shown). We expected that triggering the immune response by an immune modulator was desired and thus formulation NP4 contained the TLR9 ligand CpG oligonucleotide (10 µg.mL^{-1}). For this formulation, CpG in HEPES sucrose buffer was added to the THF solution containing peptide amphiphile PBLG$_{30}$-TAT:PBLG$_{30}$-K (9:1), ensuring the efficient incorporation of CpG into the PBLG$_{30}$-TAT/K (9:1) polypeptide NP based on attractive electrostatic interactions. All NP formulations were subsequently mixed with HA and used in all in vivo and in vitro experiments (Table 2). The final HA concentration and NP concentration in all formulations were always 10 µg.mL^{-1} and 6.77×10^{-6} M, respectively.

The self-assembled NPs were first characterized by DLS and zeta potential measurements. DLS revealed that the NP1 and NP2 formulations had comparable hydrodynamic diameters (Z av 200-240 nm), with a zeta potential of -30 mV and +20 mV, respectively (Fig. 2A). Immune modulator CpG was added during the self-assembly of NP3 to obtain NP formulation NP4. This resulted in a drop of the zeta potential from +20 mV (NP3) to -41 mV in presence of CpG (NP4), and also resulted in smaller NP (Z av of 216 nm and 160 nm, respectively). This decrease in both size and zeta potential is indicative of the tight binding of the negatively charged CpG oligonucleotides with the positively charged NP. The CpG loading was determined by measuring the adsorption of fluorescently-labeled CpG (ODN 1826-FITC, Invitrogen), showing a CpG loading efficiency between 55% and 60%. [19c]

Table 2: Formulations used in *in vitro* and *in vivo* studies, hereafter referred to as annotated.

	Short name	Composition	Z_{ave}	pdi
Nanoparticle formulations without HA	NP1 NP2 NP3 NP4	$PBLG_{30}$-K $PBLG_{30}$-TAT $PBLG_{30}$-TAT: $PBLG_{30}$-K (9:1) $PBLG_{30}$-TAT: $PBLG_{30}$-K (9:1) + CpG	210 ± 42 233 ± 69 216 ± 45 160 ± 68	0.07 ± 0.03 0.13 ± 0.09 0.14 ± 0.07 0.09 ± 0.03
Nanoparticle formulations with HA	HA/NP1 HA/NP2 HA/NP3 HA/NP4	HA/$PBLG_{30}$-K HA/$PBLG_{30}$-TAT HA/$PBLG_{30}$-TAT: $PBLG_{30}$-K (9:1) HA/$PBLG_{30}$-TAT: $PBLG_{30}$-K (9:1) + CpG	753 ± 393 799 ± 314 1210 ± 430 688 ± 457	0.24 ± 0.04 0.31 ± 0.17 0.33 ± 0.13 0.31 ± 0.07
Control formulations		HA HA/CpG HA/Al(OH)$_3$		

Z_{ave}; Z-average hydrodynamic diameter and pdi; polydispersity index obtained from dynamic light scattering measurements (n=3)

Addition of HA to the preformed NP1-4 resulted in a size increase and a significant drop in zeta potential for the two cationic nanoparticles NP2 and NP3 (Fig. 2 A). HA is a negatively charged protein that interacts with the cationic surface of the NP, resulting in the drop of the zeta potential. The adsorption efficiency of HA correlated well with the surface charge of the NP. A fluorescent labeled HA (IR Dye 800CW, Licor) was used to quantify the amount of HA associated with each NP formulation. [23] The highest amount of HA was adsorbed on cationic NP2 and NP3 (adsorption efficiency 79% and 76%, respectively), while HA association with negatively charged NP1 and NP4 was significantly lower (39% and 36%, respectively) (Fig. 2 B).
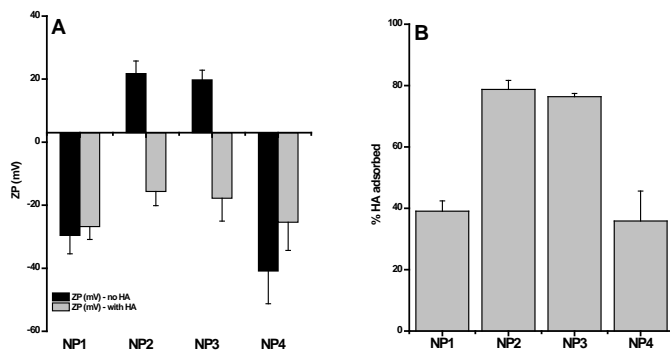
Fig. 2: (A) Zeta potential (ZP) of polypeptide-*b*-peptide NP1-4; before (■) and after HA adsorption, HA/NP1-4 (▢). Each bar represents the average of 3 different batches. **(B)** Percentage of the fluorescently labeled HA associated with HA/NP1-4. Error bars represent the standard deviation (n=3).

The morphology of the resulting assemblies was visualized using cryo electron microscopy (Cryo-EM). Cryo-EM imaging showed that NP1 self-assembled into micellar structures of approximately 200 nm in diameter (Fig. 3 A). Self-assemblies of NP2 resulted in 20-30 nm micelles and aggregation of these micelles with a typical size of 200 nm (Fig. 3 B). Next, we studied the self-assembling behavior of NP3 and we found structures resembling to those observed for NP1 as well as NP2 (Fig. 3C). Interestingly, the addition of the negatively charged CpG resulted in a better defined and more homogeneous population of NP with a diameter around 200 nm (Fig. 3 D). Moreover, a clear contrast between (CpG-containing) NP4 (Fig. 3 D) and NP3 (without CpG) (Fig. 3 C) was found, most likely because of electrostatic interactions between the surface bound CpG and the positively charged polypeptide NP. As expected, the addition of HA to the four NP formulations induced aggregation as observed by DLS. Within these aggregates, the individual NP morphology and size were maintained (Fig. 3 F-I). We also observed 10-15 nm structures on the surface of NP which are similar to those observed for free HA in solution (Fig. 3 E), presumably due to association of HA with the NP surface.
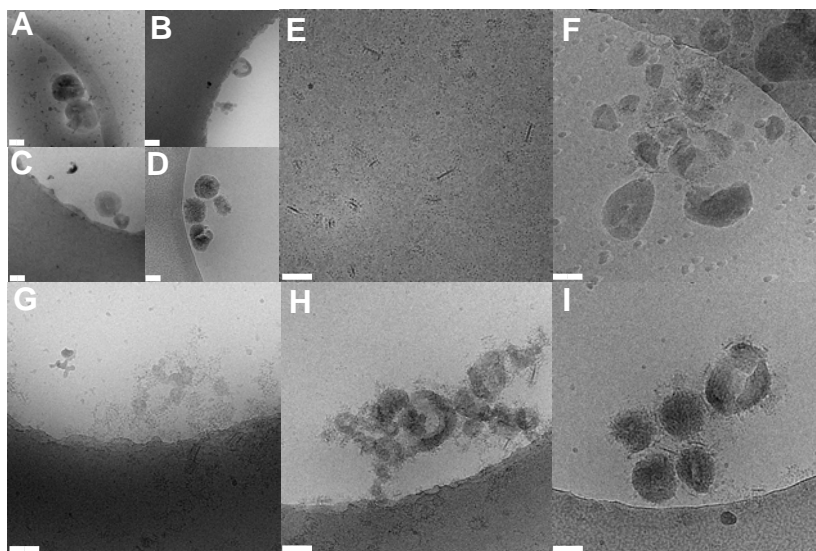
Fig. 3: Cryo-EM imaging of polypeptide-b-peptide NP. Plain NP: A) NP1, B) NP2, C) NP3, D) NP4; HA alone (E); NP mixed with 10 µg.ml^{-1} HA: F) HA/NP1, G) HA/NP2 H) HA/NP3, I) HA/NP4. Scale bar is 100 nm.

To assess the immunogenicity of the HA/NP formulations in vivo, these were injected subcutaneously in C57BL/6 mice. All mice received a first (prime) injection at day 0, and a second (boost) injection after 21 days with the same mixture. Serum was collected on day 20 and 42. HA-specific serum IgG1 (Fig. S3, Supporting Information) and IgG2a/c titers (Fig. 4 A, B) were assessed after the first (prime) and the second (boost) immunization, and HI titers, as a measure for the level of functional antibodies, were measured after the boost (Fig. 4 C). Interestingly, after boost, all HA/NP formulations induced superior levels of IgG1 compare to the antigen alone, which is consistent with the observations made in our first paper (Fig. S3-A, Supporting Information). Although, important differences were noticed, after both, prime and boost injections of the HA/NP4 formulation, as they elicited high levels of IgG2a/c compared with all the other groups, including HA mixed with the commercially available adjuvant Al(OH)$_3$ (Fig. 4 A, B), resulting in a shift of the IgG2a/c/IgG1 ratio (Fig. S3-B, Supporting Information). Increased levels of IgG2a/c indicate an enhanced Th1 response, which is in line with the superior level of interferon-γ secretion from the spleen cells collected from the mice injected with the HA/NP4 formulation (Fig. S4, Supporting Information). Moreover, the sera from mice immunized with HA/NP4 had an enhanced HI titer compared with all other groups with a significant difference compared with the non-adjuvanted HA control (p <0.05) (Fig. 4 C).

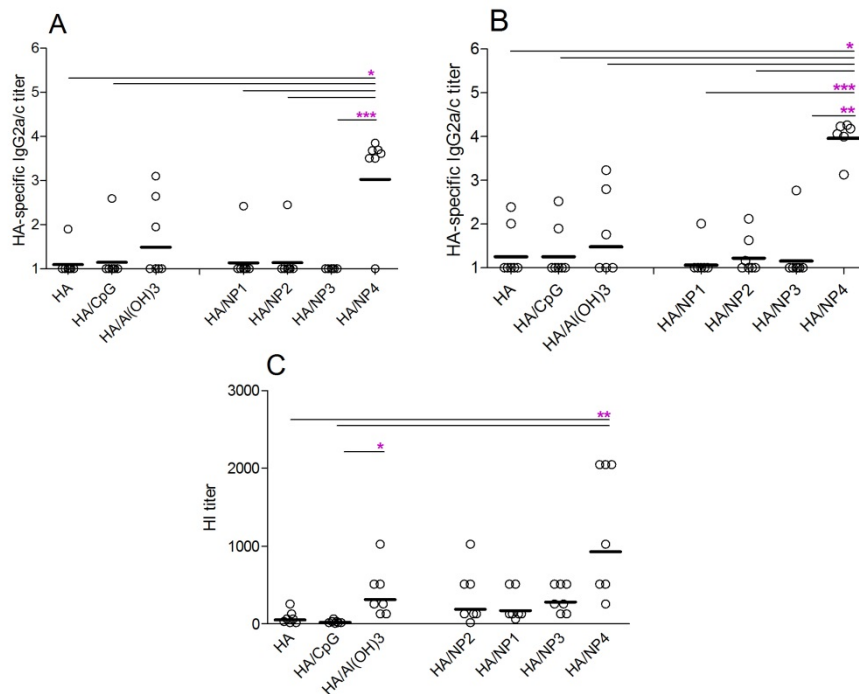**Fig. 4:** Immune response in mice after subcutaneous injection of 2.0 μg HA, free or mixed with CpG or Al(OH)$_3$ or NP formulations: HA-specific serum IgG2a/c titers after prime (A) and boost (B), and HI titers after boost (C). For panels A & B each dot represents the log serum titer of an individual mouse (non-responding mice were given an arbitrary titer of 10) bars represent the geometric mean. For panel C, each dot represents the log HI titer in serum of an individual mouse and bars represent the geometric mean. Significant difference between the groups were indicated with *, ** and *** (Respectively: $p < 0.05$, $p < 0.01$, $p < 0.001$).

Stimulation of antigen uptake by APC is important to generate a robust antiviral immune response; however, it is not the only prerequisite. Adjuvant systems should also enable a potent stimulation of the innate immune response. Therefore DC activation by the HA/NP was studied. DC derived from monocytes isolated from human donor blood were used to measure the upregulation in vitro of two maturation surface markers (MHCII and CD86) upon stimulation by the HA/NP. Cells exposed to the different HA/NP formulations showed upregulated MHCII marker levels as compared with HA. However, the increase was only significant when the DC were stimulated by NP3 containing the TAT peptide sequence. For the CD86 markers a similar trend was observed: the CpG-containing NP (HA/NP4) induced a significant upregulation as compared with HA alone. In contrast, injection of a HA/CpG solution did not yield an increase in CD86 marker expression (Fig. 5), showing the cooperative effect of CpG and PbP-A NP.
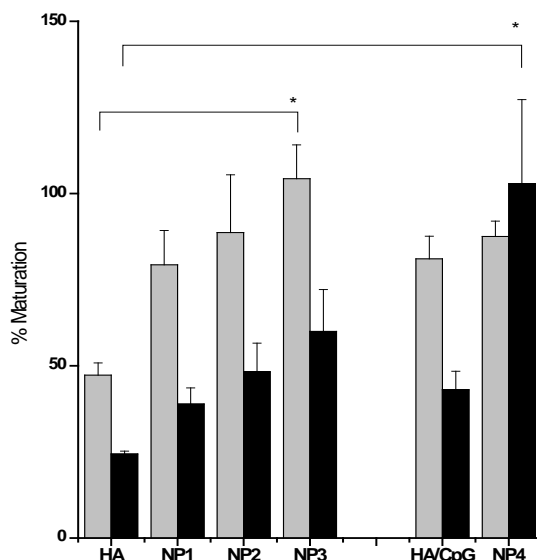
Fig. 5: Upregulation of the MHC II (☐) and CD86 (■) DC maturation markers induced by the various polypeptide-b-peptide NP formulations versus free HA; relative to the 100 ng.mL^{-1} LPS control group. Error bar represents SEM (n=3). Significant difference between the polypeptide-b-peptide NP formulation and free HA are indicated with * (p < 0.05).

In summary, we have synthesized two new peptide amphiphiles, PBLG$_{30}$-TAT and PBLG$_{30}$-K, and demonstrated their ability to self-assemble into cationic NP in various formulations. Co-delivery of CpG with HA/NP (HA/NP4) resulted in an enhanced immune response in mice against the HA antigen, towards a Th1 response (as reflected by elevated levels of IgG2a/c). A Th1 response is important to target intracellular pathogens, thus opening an avenue for vaccine development against viral pathogens. This formulation also demonstrated a higher immunogenicity when compared with the commonly used adjuvant Al(OH)$_3$. Further studies are required to obtain a better understanding of the self-assembly of the polypeptide amphiphiles and the effect of the resulting NP on the immunogenicity of associated antigens.

References

1. D. Missirlis , A. Chworos , C. J. Fu , H. A. Khant , D. V. Krogstad , M. Tirrell , Langmuir 2011 , 27 , 6163 .
2. a) H. G. Cui , M. J. Webber , S. I. Stupp , Biopolymers 2010 , 94 , 1 ; b) R. Solaro , M. Alderighi , M. C. Barsotti , A. Battisti , M. Cifelli , P. Losi , R. Di Stefano , L. Ghezzi , M. R. Tine , J. Bioact. Compat. Pol. 2013 , 28 , 3 .
3. D. W. P. M. Lowik , J. C. M. van Hest , Chem. Soc. Rev. 2004 , 33 , 234 .
4. S. G. Zhang , Nat. Biotechnol. 2003 , 21 , 1171 .
5. a) J. D. Hartgerink , E. Beniash , S. I. Stupp , Science 2001 , 294 , 1684 ; b) J. D. Hartgerink , E. Beniash , S. I. Stupp , Proc. Natl. Acad. Sci. U. S. A. 2002 , 99 , 5133 .
6. a) S. Cavalli , F. Albericio , A. Kros , Chem. Soc. Rev. 2010 , 39 , 241 ; b) S. Cavalli , J. W. Handgraaf , E. E. Tellers , D. C. Popescu , M. Overhand , K. Kjaer , V. Vaiser , N. A. J. M. Sommerdijk , H. Rapaport , A. Kros , J. Am. Chem. Soc. 2006 , 128 , 13959 ; c) H. Robson Marsden , N. A. Elbers , P. H. Bomans , N. A. Sommerdijk , A. Kros , Angew. Chem. Int. Ed. 2009 , 48 , 2330 ; d) P. Berndt , G. B. Fields , M. Tirrell , J. Am. Chem. Soc. 1995 , 117 , 9515 .
7. a) A. Rosler , H. A. Klok , I. W. Hamley , V. Castelletto , O. O. Mykhaylyk , Biomacromolecules 2003 , 4 , 859 ; b) P. Wilke , H. G. Borner , ACS Macro Lett. 2012 , 1 , 871 ; c) H. R. Marsden , A. V. Korobko , E. N. M. van Leeuwen , E. M. Pouget , S. J. Veen , N. A. J. M. Sommerdijk , A. Kros , J. Am. Chem. Soc. 2008 , 130 , 9386 ; d) R. Matmour , I. De Cat , S. J. George , W. Adriaens , P. Leclere , P. H. H. Bomans , N. A. J. M. Sommerdijk , J. C. Gielen , P. C. M. Christianen , J. T. Heldens , J. C. M. van Hest , D. W. P. M. Lowik , S. De Feyter , E. W. Meijer , A. P. H. J. Schenning , J. Am. Chem. Soc. 2008 , 130 , 14576 ; e) F. Checot , S. Lecommandoux , H. A. Klok , Y. Gnanou , Eur. Phys. J. E. 2003 , 10 , 25 ; f) N. Dube , A. D. Presley , J. Y. Shu , T. Xu , Macromol. Rapid Commun. 2011 , 32 , 344 ; g) A. R. Rodriguez , U. J. Choe , D. T. Kamei , T. J. Deming , Macromol. Biosci. 2012 , 12 , 805 ; h) H. A. Klok , J Polym. Sci. Polym. Chem. 2005 , 43 , 1 ; i) H. Robson Marsden , A. Kros , Macromol. Biosci. 2009 , 9 , 939 .
8. a) J. J. L. M. Cornelissen , M. Fischer , N. A. J. M. Sommerdijk , R. J. M. Nolte , Science 1998 , 280 , 1427 ; b) M. J. Boerakker , J. M. Hannink , P. H. H. Bomans , P. M. Frederik , R. J. M. Nolte , E. M. Meijer , N. A. J. M. Sommerdijk , Angew. Chem. Int. Ed. 2002 , 41 , 4239 ; c) G. W. M. Vandermeulen , C. Tziatzios , H. A. Klok , Macromolecules 2003 , 36 , 4107 ; d) G. W. M. Vandermeulen , H. A. Klok , Macromol. Biosci. 2004 , 4 , 383 ; e) J. Babin , J. Rodriguez-Hernandez , S. Lecommandoux , H. A. Klok , M. F. Achard , Faraday Discuss. 2005 , 128 , 179 ; f) G. W. M. Vandermeulen , C. Tziatzios , R. Duncan , H. A. Klok , Macromolecules 2005 , 38 , 761 ; g) F. Checot , S. Lecommandoux , Y. Gnanou , H. A. Klok , Angew. Chem. Int. Ed. 2002 , 41 , 1339 ; h) J. A. Hanson , Z. Li , T. J. Deming , Macromolecules 2010 , 43 , 6268 .
9. a) L. Liu , K. Xu , H. Wang , P. K. Jeremy Tan , W. Fan , S. S. Venkatraman , L. Li , Y.-Y. Yang , Nat. Nanotechnol. 2009 , 4 , 457 ; b) M. J. Webber , J. Tongers , M. A. Renault , J. G. Roncalli , D. W. Losordo , S. I. Stupp , Acta Biomater. 2010 , 6 , 3 ; c) V. Z. Sun , Z. Li , T. J. Deming , D. T. Kamei , Biomacromolecules 2011 , 12 , 10 .
10. S. R. Bull , M. O. Guler , R. E. Bras , T. J. Meade , S. I. Stupp , Nano Lett. 2005 , 5 , 1 .
11. a) R. G. Ellis-Behnke , G. E. Schneider , Methods Mol. Biol. 2011 , 726 , 259 ; b) A. P. Nowak , V. Breedveld , L. Pakstis , B. Ozbas , D. J. Pine , D. Pochan , T. J. Deming , Nature 2002 , 417 , 424 ; c) L. M. Pakstis , B. Ozbas , K. D. Hales , A. P. Nowak , T. J. Deming , D. Pochan , Biomacromolecules 2004 , 5 , 312 .
12. M. Black , A. Trent , Y. Kostenko , J. S. Lee , C. Olive , M. Tirrell , Adv. Mater. 2012 , 24 , 3845 .
13. a) J. S. Rudra , Y. F. Tian , J. P. Jung , J. H. Collier , Proc. Natl. Acad. Sci. U. S. A. 2010 , 107 , 622 ; b) G. A. Hudalla , J. A. Modica , Y. F. Tian , J. S. Rudra , A. S. Chong , T. Sun , M. Mrksich , J. H. Collier , Adv. Healthc. Mater. 2013 , 2 , 1114.
14. a) Q. B. Meng , Y. Y. Kou , X. Ma , Y. J. Liang , L. Guo , C. H. Ni , K. L. Liu , Langmuir 2012 , 28 , 5017 ; b) H. R. Marsden , A. V. Korobko , E. N. van Leeuwen , E. M. Pouget , S. J. Veen , N. A. Sommerdijk ,

A. Kros , J. Am. Chem. Soc. 2008 , 130 , 9386 ; c) H. R. Marsden , J. W. Handgraaf , F. Nudelman , N. A. J. M. Sommerdijk , A. Kros , J. Am. Chem. Soc. 2010 , 132 , 2370 .

15.   a) M. Zhao , R. Weissleder , Med. Res. Rev. 2004 , 24 , 1 ; b) F. Porta , G. E. M. Lamers , J. I. Zink , A. Kros , Phys. Chem. Chem. Phys. 2011 , 13 , 9982 ; c) C. C. Berry , Nanomedicine 2008 , 3 , 357 ; d) V. P. Torchilin , Adv. Drug Delivery Rev. 2008 , 60 , 548 .

16.   M. Singh , A. Chakrapani , D. O'Hagan , Expert Rev. Vaccines 2007 , 6 , 797 .

17.   R. Sawant , V. Torchilin , Methods Mol. Biol. 2011 , 683 , 431 .

18.   N. A. Christian , M. C. Milone , S. S. Ranka , G. Z. Li , P. R. Frail , K. P. Davis , F. S. Bates , M. J. Therien , P. P. Ghoroghchian , C. H. June , D. A. Hammer , Bioconjugate Chem. 2007 , 18 , 31 .

19.   a) S. Kamstrup , T. H. Frimann , A. M. Barfoed , Antiviral Res. 2006 , 72 , 42 ; b) B. Slütter , W. Jiskoot , J. Controlled Release 2010 , 148 , 117 ; c) B. Slütter , S. M. Bal , Z. Ding , W. Jiskoot , J. A. Bouwstra , J. Controlled Release 2011 , 154 , 123 ; d) L. Dong , I. Mori , M. J. Hossain , B. Liu , Y. Kimura , J. Gen. Virol. 2003 , 84 , 1623 .

20.   D. M. Klinman , Int. Rev. Immunol. 2006 , 25 , 135 .

21.   H. R. Marsden , C. B. Quer , E. Y. Sanchez , L. Gabrielli , W. Jiskoot , A. Kros , Biomacromolecules 2010 , 11 , 833 .

22.   H. R. Marsden , L. Gabrielli , A. Kros , Polym. Chem. 2010 , 1 , 1512 .

23.   C. B. Quer , H. R. Marsden , S. Romeijn , H. Zope , A. Kros , W. Jiskoot , Polym. Chem. 2011 , 2 , 1482 .

24.   E. Schlosser , M. Mueller , S. Fischer , S. Basta , D. H. Busch , B. Gander , M. Groettrup , Vaccine 2008 , 26 , 1626 .

25.   S. M. Bal , S. Hortensius , Z. Ding , W. Jiskoot , J. A. Bouwstra , Vaccine 2011 , 29 , 1045 .

Supplementary information

1. Abbreviations

ANOVA, analysis of variance; APC, antigen-presenting cells; BLG-NCA, γ-benzyl L-glutamate N-carboxyanhydride; BSA, bovine serum albumin; CpG, bacterial cytosine phosphodiester guanine oligomer; DIPEA, N,N-diisopropylethylamine; DC, dendritic cells; DCM, dichloromethane; DIPEA, N,N-diisopropylethylamine; DMF, N,N-dimethylformamide; DMSO, dimethyl sulfoxide; ELISA, enzyme-linked immunosorbent assay; NMP, N-methyl-2-pyrrolidone; FCS, fetal calf serum; FITC, fluorescein isothiocyanate; FMOC, 9-fluorenylmethoxycarbonyl; GPC, gel permeation chromatography; HA, hemagglutinin; HBSS, Hank's balanced salt solution; HCTU, O-(6-chlorobenzotriazol-1-yl)-N,N,N′,N′-tetramethyluronium hexafluorophosphate; HEPES, 4-(2-hydroxyethyl)-1-piperazine-ethanesulfonic acid; ^{1}H-NMR, ^{1}H nuclear magnetic resonance; HPLC, high-pressure liquid chromatography; HRP, horseradish peroxidase; Ig, immunoglobulin; LC-MS, liquid chromatography–mass spectrometry; MTT, 3-(4,5-Dimethylthiazol-2-yl)-2,5-diphenyltetrazolium bromide; NMP, 1-methyl-2-pyrrolidinone; NP, nanoparticles; PbP-A, polypeptide-b-peptide amphiphiles; PDI, polydispersity index; THF, tetrahydrofuran; Cryo-EM, cryogenic electron microscopy; TFA, trifluoroacetic acid; TIS, triisopropyl silane.

2. Materials and Methods

Fmoc protected amino acids and peptide synthesis grade DMF, DCM and NMP solvents were obtained from BioSolve Ltd. Sieber amide resin was purchased from Iris Biotech GmbH, Germany. Influenza hemagglutinin antigen (H3N2 Wisconsin strain) was obtained from Solvay (Weesp, The Netherlands). BSA was purchased from Merck (Darmstadt, Germany). ELISA plates were obtained from Greiner (Alphen a/d Rijn, The Netherlands). HRP conjugated goat anti-mouse IgG (γ chain specific), IgG1 (γ1 chain specific) and IgG2a (γ2a chain specific) were ordered from Southern Biotech (Birmingham, USA). Chromogen 3,3′,5,5′-tetramethylbenzidine (TMB), GM-CSF and interleukin-4 (IL4), were provided by Biosource-Invitrogen (Breda, The Netherlands). HBSS, FCS and all culture media, including penicillin/streptomycin (PEST) and trypsin were supplied from Gibco (Invitrogen, Carlsbad, CA). Nimatek® (100 mg.mL^{-1} ketamine, Eurovet Animal Health B.V., Bladel, The Netherlands) and Rompun® (20 mg.mL^{-1} xylazine, Bayer B.V.,Mijdrecht, The Netherlands) were obtained from the pharmacy of Leiden University Medical Center. HEPES, DCM, DMSO, MTT and other chemicals were acquired from Sigma-Aldrich (Zwijndrecht, The Netherlands), unless stated otherwise.

3. Solid-Phase Peptide Synthesis of Peptide "K" and "TAT"

Peptide "K" and "TAT" were prepared following standard Fmoc chemistry on sieber amide resin using Liberty-1 (CEM corporation, Matthews, NC, United States) microwave assisted automated peptide synthesizer. Scale of synthesis was 0.25

mmol and activation of amino acid derivatives was achieved using HCTU/DIPEA. After the peptide "K" and "TAT" were prepared, the resin was removed from the reaction vessel, The amount of successfully synthesized "K" and "TAT" was estimated using the mass added to the resin during the synthesis, and by integration of HPLC peaks from an LC-MS run of a test cleavage of 10 mg of resin-bound peptide using TFA/TIS/water; 95/2.5/2.5 (v/v).
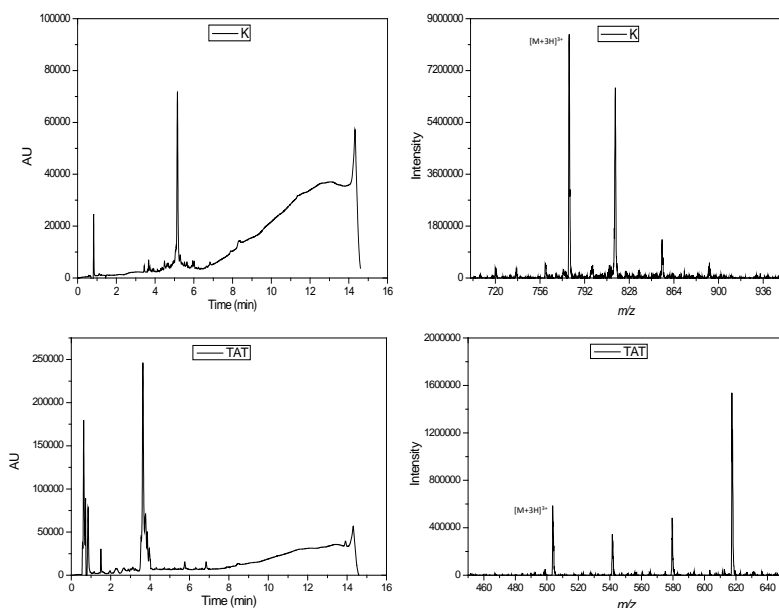

Fig. S1: HPLC traces of peptide K (with 67% purity) and peptide TAT (with 60% purity) along with mass observed for main peak and corresponding TFA adducts.

4.   Solid-Phase Synthesis of Poly(γ-benzyl L-glutamate)-block-K (PBLG-K) and Poly(γ-benzyl L-glutamate)-block-TAT (PBLG-TAT)

γ-benzyl L-glutamate N-carboxyanhydride was synthesized and characterized as described previously.[1] The poly(γ-benzyl L-glutamate) block was synthesized on the solid phase using one-pot NCA polymerization of BLG-NCA initiated from the N-terminus amine of resin-bound peptide "K" or "TAT". The resin-bound peptide was dried overnight in vacuum oven at 37 °C, and then placed in argon atmosphere for 5 h. Next, under an argon atmosphere, the peptide bound 0.25 mmol resin was swollen in dry DCM. Subsequently the appropriate weight of NCA (determined from the mass loading and HPLC peak integration) was added. [1] The flask was shaken for 48 h. The resin was drained and washed extensively with DCM to wash away the homopolymer formed during the reaction. The yields of the resin-bound block co-polypeptides were 50-60%. While keeping the side chains of the peptides intact, PBLG-Peptide "K" or "TAT" hybrid block copolymer was cleaved from the resin using

TFA:DCM (1:99) (v/v) for 2 min, 10 times. Each cleavage mixture was precipitated in cold methanol and centrifuged to obtain pellets. Pellets were washed 3 times using cold methanol and vacuum-dried. The protecting groups of peptide "K" and "TAT" were removed using TFA:DCM:water:TIS; 47.5:47.5:2.5:2.5 (v/v) for 3 h. The product was precipitated drop wise in cold methanol and centrifuged. Further 3 washes of cold methanol were performed. The product was vacuum dried to obtain both block copolymers in 20-25% in yield.

5. Characterization of the PBLG-K and PBLG-TAT Polypeptide-b-Peptides

Molecular weights and polydispersity index (PDI) of the protected PBLG-K and PBLG-TAT PbP-A were determined using gel phase chromatography (GPC). GPC analyses were performed using a Shimadzu system and a Polymer Laboratories column (3M-RESI-001-74, 7.5 mm diameter, 300 mm length). To prevent aggregation, DMF was used as the eluent at 60 °C with a flow rate of 1 mL.min^{-1}. Molecular weights were calibrated using polystyrene standards.
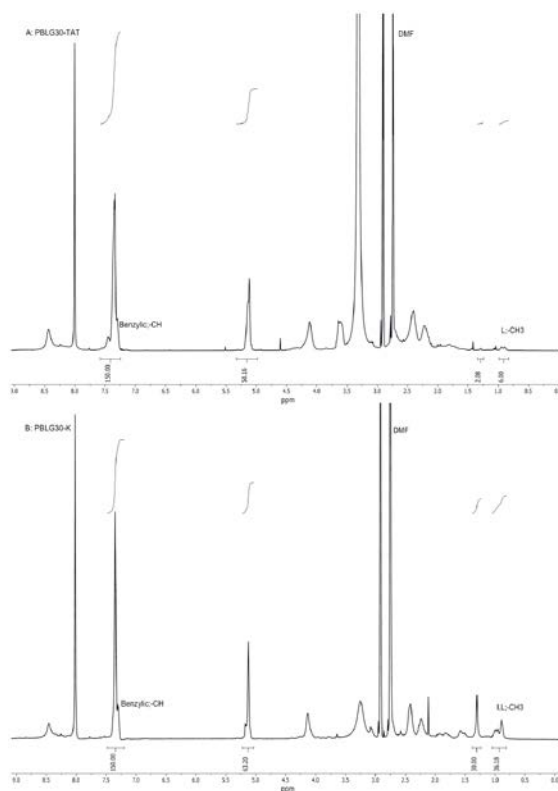

Fig. S2:. ^{1}H NMR spectrum of PBLG$_{30}$-TAT (A) and PBLG$_{30}$-K (B) in N,N-dimethylformamide-d7 (DMF-d7) at 60 °C. By comparing benzylic -CH with respective leucine or leucine/isoleucine -CH3 peak, an average degree of polymerization of 30 was estimated for both block copolymers. The high intensity signal at 3.3 ppm for PBLG$_{30}$-TAT is due to residual water.

6. Preparation of PBLG$_{30}$-K and PBLG$_{PBLG}$-TAT Nanoparticles

The nanoparticles (NP) were prepared by a solvent evaporation method as described previously.[2] Briefly, the polymer (0.02 µmol) was dissolved in 2 ml THF in a 50 ml round flask, then 3 ml of HEPES sucrose buffer (HEPES 20 mM, sucrose 10% (w/w), pH 7.4) was added all at once to the polymer solution, and the mixture was homogenized by vortexing for 1 minute (200 rpm). Immediately, the THF was removed by rotary evaporation at 30 kPa, 25°C for 10 minutes. The CpG loaded NP were prepared by using the same method, but with HEPES sucrose buffer containing 10 µg.mL^{-1} CpG. Finally, the HA/NP were prepared extemporaneously, by mixing (prior to the injection) the proper volumes of HA stock solution (453 µg.mL^{-1}) to the preformed polypeptide NP suspension (Unbound HA was not removed and the final HA concentration was 10 µg.mL^{-1}).

7. Size, Charge and Morphology Characterization of the Polypeptide Nanoparticles

Particle size distributions were determined by means of dynamic light scattering (DLS) using a NanoSizer ZS (Malvern Instruments). The zeta potential of the particles was measured by laser Doppler electrophoresis on the same instrument.

Samples for cryo-EM were concentrated by centrifuging using Amicon Ultra, Ultracel®-100K (regenerated cellulose 100,000 MWCO, Millipore, Ireland) at room temperature. HA was added to the samples just before the vitrification process. Typically 10 µg.mL^{-1} concentration of HA is used during the experiments therefore for imaging concentration of HA was adjusted to the resulting centrifuged sample. Sample stability was verified by DLS and TEM. Cryo-EM measurements were performed on a FEI Technai 20 (type Sphera) transmission electronmicroscope or on a Titan Krios (FEI). A Gatan cryo-holder operating at ~ -170 °C was used for the cryo-EM measurements. The Technai 20 was equipped with a LaB6 filament operating at 200 kV, and the images were recorded using a 1k × 1k Gatan CCD camera. The Titan Krios was equipped with a field emission gun (FEG) operating at 300 kV. Images were recorded using a 2k × 2k Gatan CCD camera equipped with a post column Gatan energy filter (GIF). The sample vitrification procedure was carried out using an automated vitrification robot: a FEI Vitrobot Mark III. TEM grids, both 200 mesh carbon coated copper grids and R2/2 Quantifoil Jena grids, were purchased from Aurion. Copper grids bearing lacey carbon films were homemade using 200 mesh copper grids from Aurion. Grids were treated with a surface plasma treatment using a Cressington 208 carbon coater operating at 25 A for 40 s prior to the vitrification procedure.

8. Quantification of HA and CpG Associated with the Nanoparticles

Estimation of the HA adsorption onto the nanoparticles was done as described previously [3]. For this study we used labeled HA (IRDye® 800CW, Licor). Briefly, the HA/NP complexes and the free HA were filtered through polycarbonate membranes (Whatman, Nucleopore) of 0.2 µm pore size, using an extruder (T001 10

ml, Thermobarrel Extruder Lipex Biomembrane). Under these conditions the NP are retained on the filter and HA passes through. The amount of HA, remaining in the filtrate, was quantified with an Infinite M1000 microplate reader (Tecan).

The amount of CpG present in the NP was determined using fluorescently labeled analogs (10% of used CpG were labeled), as described previously [4]. Free TLR ligand was separated from the NP by filtration using an Amicon Ultra, Ultracel®-100K (Regenerated cellulose 100000 MWCO, Millipore, Ireland) and quantified using a FS920 fluorimeter (Edinburgh Instruments, Campus Livingston, UK).

9. DC Maturation Assay

Monocytes isolated from buffy coats (Sanquin, Amsterdam, The Netherlands) were cultivated to differentiate into immature DC, as described previously. DC were incubated for 48 h at 37°C in RPMI 1640, containing 500 U/ml GM-CSF and 100 U/ml IL4, with 100 µl volume of HA/NP suspension in 1 ml cell culture medium, and LPS (100 ng.mL^{-1} cell culture medium) was used as a positive control. Cells were washed 3 times with PBS containing 1% (w/v) BSA and 2% (v/v) FBS and incubated for 30 min with a mixture of 50× diluted anti-HLADR-FITC or anti-CD86-APC (Becton Dickinson) on ice, to measure the expression of MHCII or CD86, respectively, on the surface of the DC. Cells were washed and expression of the surface markers was quantified by using flow cytometry (FACSCanto, BD Biosciences, San Jose, CA, USA). Live cells were gated based on forward and side scatter. The upregulation of the two surface markers by 100 ng.mL^{-1} LPS was set as 100%. A minimum of 10,000 gated cells were analyzed in each experiment.

10. In vivo Experiments

Female C57-BL/6 mice, 8-weeks old at the start of the vaccination study, were purchased from Charles River Laboratories International, Wilmington, MA, USA, and maintained under standardized conditions in the animal facility of the Leiden Academic Centre for Drug Research, Leiden University. The study was carried out under the guidelines compiled by the Animal Ethic Committee of The Netherlands. The mice received two subcutaneous injections of 200 µl vaccine (2 µg HA/injection): a prime (day 1) and a boost (day 21). The antigen was either injected alone or mixed with NP to the final concentration of 10 µg HA/ml of NP solution. Unbound HA was not removed and each mouse received the same amount of HA and NP. Blood samples were taken one day before prime and boost, and 3 weeks after the boost. IgG titers were determined by ELISA.

The IgG subtype profile of influenza-specific antibodies was checked on day 20 and 42 by sandwich ELISA as previously described. Briefly, ELISA plates (Greiner Bio-One B.V., The Netherlands) were coated overnight at 4°C with 100 ng HA/well in coating buffer (0.05 M sodium carbonate/bicarbonate, pH 9.6). Plates were subsequently washed twice with PBS containing 0.05% Tween 20, pH 7.2 (PBST) and then blocked by incubation with 1% (w/v) BSA in PBST for 1 h at 37°C. Thereafter the plates were washed three times with PBST. Two-fold serial dilutions

of sera from individual mice were applied to the plates and incubated for 1.5 h at 37°C. Plates were incubated with HRP-conjugated goat antibodies against either mouse IgG1 or IgG2a (Invitrogen, The Netherlands) for 1 h at 37°C. After washing, plates were incubated with TMB and the reaction was stopped with sulfuric acid (2 M). The detection was achieved by measuring optical density at 450 nm. C57BL/6 mice express the Igh1-b gene, which encodes the IgG2c isotype rather than IgG2a. However, here we used an anti-IgG2a isotype (which cross-reacts with IgG2c[5] and titers are reported as IgG2a/c titers. Finally, antibody titers were expressed as the reciprocal of the sample dilution that corresponds to half of the maximum absorbance at 450 nm of a complete s-shaped absorbance–log dilution curve.
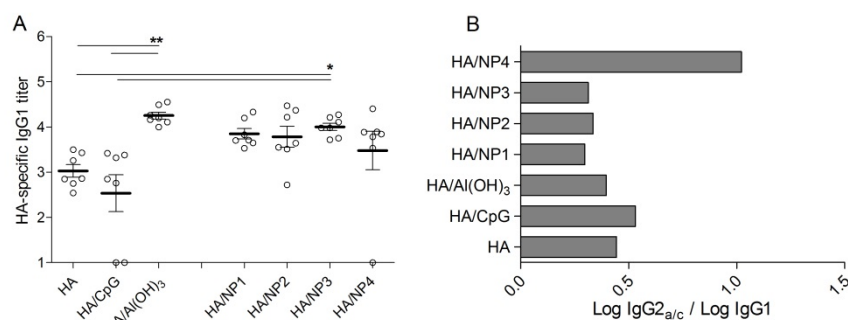

Fig.S3: Immune response in mice after subcutaneous injection of HA/NP; (A): HA-specific serum IgG1 titers after boost, each dot represents the log serum titer of an individual mouse (non-responding mice were given an arbitrary titer of 10) bars represent the geometric mean and significant difference between the groups were indicated with * and ** (Respectively: $p < 0.05$, $p < 0.01$). (B): Corresponding average Log IgG 2 a/c/Log IgG1 ratio, indicative of the quality of the immune response.

11. Hemagglutination Inhibition Assay

Hemagglutination inhibition (HI) titers in serum were determined as described previously. [3] Briefly, serum was inactivated at 56°C for 30 min. In order to reduce nonspecific hemagglutination, 25% kaolin suspension was added to inactivate sera. After centrifugation at 1,200×g, 50 µL of the supernatant was transferred in duplicate to 96-well round-bottom plates (Greiner) and serially diluted twofold in PBS. Then, four hemagglutination units of A/Wisconsin influenza inactivated virus were added to each well, and the plates were incubated for 40 min at room temperature. Finally, 50 µL of 1% guinea pig red blood cells (Harlan Scientific, The Netherlands) diluted in PBS, were added to each well and incubated for 2 h at room temperature. The highest dilution capable of preventing hemagglutination was scored as the HI titer.

All the data of the in vitro studies were analyzed with a one-way analysis of variance (ANOVA) with Bonferroni's post-test. Regarding the in vivo data, Antibody titers were logarithmically transformed before statistical analysis. A one-way ANOVA with

a Kruskal Wallis post-test analysis was performed in order to demonstrate significant differences between the experimental groups, the statistical analysis was carried out using Graphpad Prism software and a p value less than 0.05 was considered to be significant.
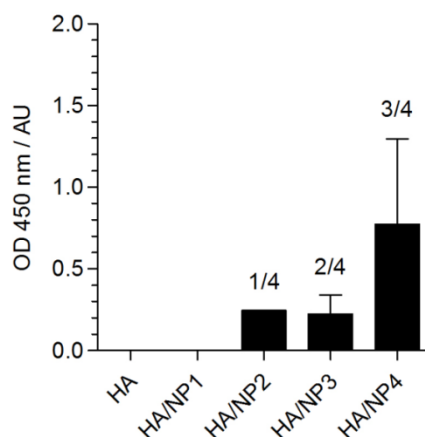

Fig.S4: IFN gamma levels secreted by spleen cells collected from mice exposed to HA alone and HA/NP formulations.

References

1. H. R. Marsden, J. W. Handgraaf, F. Nudelman, N. A. J. M. Sommerdijk, A. Kros, J. Am. Chem. Soc. 2010, 132, 2370-2377.
2. H. R. Marsden, L. Gabrielli, A. Kros, Polymer Chemistry 2010, 1, 1512-1518.
3. C. Barnier Quer, H. Robson Marsden, S. Romeijn, H. Zope, A. Kros, W. Jiskoot, Polymer Chemistry 2011, 2, 1482-1485.
4. S. M. Bal, S. Hortensius, Z. Ding, W. Jiskoot, J. A. Bouwstra, Vaccine 2011, 29, 1045-1052.
5. R. M. Martin, J. L. Brady, A. M. Lew, J. Immunol. Methods 1998, 212, 187-192.